International Journal of Applied Earth Observations and Geoinformation 96 (2021) 102282

Contents lists available at ScienceDirect

International Journal of Applied Earth Observations and Geoinformation

journal homepage: www.elsevier.com/locate/jag

Leaf area index estimation using top-of-canopy airborne RGB images

Rahul Raj [a,*], Jeffrey P. Walker [b], Rohit Pingale [c], Rohit Nandan [c], Balaji Naik [d], Adinarayana Jagarlapudi [c]

[a] IITB-Monash Research Academy, India
[b] Monash University, Melbourne, Australia
[c] Indian Institute of Technology Bombay, India
[d] Jayashankar Telangana State Agricultural University, India

ARTICLE INFO

Keywords:
Leaf area index
Drone-based imaging
Precision agriculture
VLADF

ABSTRACT

Leaf Area Index (LAI) is one of the most important biophysical properties of a crop, used in detecting long-term water stress, estimating biomass, and identifying crop growth stage. Remote sensing based LAI estimation techniques perform well for early growth stages but tend to produce high error during the crop reproductive stage due to canopy closure. Moreover, estimation of the true LAI from individual leaf measurements remains a challenge. Consequently, two alternate methods have been developed and compared for estimating the LAI of a maize crop using top-of-canopy RGB images collected throughout the growing season using a hexacopter. Both methods used the RGB images to estimate the canopy height and the green-canopy cover together with a 'vertical leaf area distribution factor' (*VLADF*) from allometric relations (using crop height from RBG images and days after sowing). The first method used an empirical approach to estimate the LAI from training a linear function of the above inputs to Licor canopy analyser values of LAI. The method was trialled for a research farm located in a semi-arid area of southern peninsula India and found to have validation results with an R^2 of 0.84 and RMSE of 0.36 for the unused portion of the Rabi (post-monsoon) season data of 2018–19, and R^2 of 0.77 and RMSE of 0.45 for the Rabi 2019–20 season data when compared with Licor LAI values. While seemingly acceptable, the Licor canopy analyser gives a foliage area index and so the accuracy of this model was very low (R^2 of 0.56 and RMSE of 1.34) when evaluated with true LAI from manual measurements of the leaf area. Consequently, a refinement was introduced using only *VLADF*, green-canopy cover estimates from the RBG images, and a field measured top leaf angle. The output derived from this conceptual model had an R^2 of ~0.6 and RMSE of 0.73 when compared with the true LAI values. Importantly, the LAI from this conceptual model was found to be unaffected by canopy closure during the reproductive stage of the crop.

1. Introduction

Leaf Area Index (LAI) is a biophysical property that reflects the health of the crop (Bryson et al., 1997). It largely depends on the crop growth stage, crop height, architecture of the leaves and density of the plants (Vose et al., 1994), but can also be affected by short-term water stress due to leaf rolling (Chen et al., 1992). Importantly, an increase in the LAI represents an increase in the leaf stomatal area and thus gaseous exchanges between the crop and the vegetation (Patanè, 2011). Accordingly, various crop models use LAI to calculate 'light use efficiency' of the vegetation and to simulate the energy balance equations, and to enable understanding of the physical processes that occur between plants and the environment (Bonan et al., 1993; Running et al., 1988; Qu et al., 2016; Drewry et al., 2010).

The most accurate method to find the LAI of any area is termed the 'direct method', involving the destructive sampling of leaves, which is very time consuming and labour-intensive (Dufrêne et al., 1995; Behera et al., 2010). Conversely, indirect methods are approximations and so use terms like foliage area index, effective plant area index (Garrigues et al., 2008), vegetation area index (Fassnacht et al., 1994), effective leaf area index (Chen et al., 1991) etc. However, the term 'LAI' is often used in the case of indirect measurements, even though indirect methods are affected by non-leafy parts of the canopy. Fortuitously, it has been shown that the LAI obtained from instruments such as the Licor-2000 or

* Corresponding author at: Agroinformatics Lab, CSRE, IIT Bombay, Mumbai, Maharashtra, India.
E-mail addresses: Rahul.Rahulraj@monash.edu (R. Raj), Jeff.Walker@monash.edu (J.P. Walker), Rohitpingale103@iitb.ac.in (R. Pingale), Rohitnandan@iitb.ac.in (R. Nandan), Adi@csre.iitb.ac.in (A. Jagarlapudi).

https://doi.org/10.1016/j.jag.2020.102282
Received 16 September 2020; Received in revised form 3 December 2020; Accepted 7 December 2020
Available online 22 December 2020

Licor-2200 canopy analyser is correlated with LAI measurements from the direct method (Stroppiana et al., 2006; Liu et al., 2010). However, literature shows that it is difficult to estimate the true LAI from indirect techniques at the reproductive stage (Raj et al., 2020) because of canopy closure resulting in signal saturation (Bendig et al., 2015).

In the case of maize, the canopy closure may occur between the late vegetative stage and the silking stage of the crop (Martin et al., 2007). Accordingly, only minimal changes in the top of the canopy are visible through RGB images due to canopy closure, and so these images do not represent the changes occurring inside the canopy. For example, the top layer of the canopy does not change much during the dough stage but the leaves in the bottom layer of the canopy start drying (Valentinuz et al., 2004). Accordingly, the early drying process of bottom leaves with respect to top leaves results in a decrease in LAI of the canopy. While these canopy changes are not immediately obvious from top-of-canopy observations in the visible spectrum, they can to some extent be estimated from the infrared spectrum due to changes in the chemical properties of the crop from stage to stage (Raychaudhuri et al., 2007).

Some examples of use of visible and infrared data for LAI mapping studies based on UAV technology include Duan et al. (2019), who have used visible and near-infrared multiband data to find the true LAI of rice crops using the Fourier spectral energy percentage method. The R^2 and RMSE between the estimated and true LAI was found to be around 0.75 and 1.22, respectively. However, the algorithm showed saturation of the NDVI during canopy closure. In another research, Li et al. (2019) used UAV-based high resolution RGB imagery to estimate the true LAI of a rice crop using various machine learning approaches on derived color indices and image texture. The random forest algorithm showed the best result with an R^2 and RMSE of 0.84 and 0.87, respectively. Further, Tian et al. (2017) has compared the mangrove foliage LAI (ground truth collected using a Licor-2200 plant canopy analyser) obtained from Worldview-2 imagery and UAV-based multispectral data. The linear regression model implemented on the indices dataset shown improved results in the case of UAV data, with an R^2 and RMSE of 0.817 and 0.423, respectively. In another research, Tao et al. (2020) used drone-based hyperspectral data to estimate winter wheat LAI through vegetation indices and red-edge parameters. The best result was obtained from a partial least square regression algorithm with R^2 and RMSE ranging from 0.64 to 0.76 and 0.45–0.96, respectively in various growth stages. Mathews and Jensen (2013) used a complex technique called structure from motion (SfM), in which drone-based RGB images were processed to get height metrics that were then correlated with foliage LAI of a vineyard canopy. The model performed with R^2 and RMSE of 0.56 and 0.23, respectively. Despite these studies showing that fusion of different data types can help identify changes in vegetation and thus improve LAI estimation, the RMSE of these methods remain high, limiting their use for farm-level decisions (Kimm et al., 2020). To overcome such limitations, this paper has developed a new method for estimating the LAI of maize crops from top-of-canopy drone-based RGB images using derived crop height, green-canopy cover, and a 'vertical leaf area distribution factor' (*VLADF*) lookup table.

2. Materials and methods

In this study, both an empirical and conceptual model are developed, with inputs of 1) height of the canopy; 2) green-canopy cover (GCC) and 3) the *VLADF*, which connects the top leaf area to the bottom part of the canopy leaf area. Data on the structural properties of the crop (top leaf angles, and plant leaf area at different crop height and at different growth stages) was intensively collected for two years and used here for development of the *VLADF*. The height of the canopy was derived from a digital surface model (DSM) of the farm. The DSMs were generated using Agisoft® Metashape software (AgiSoft PhotoScan Professional, 2016). GCC was estimated through a green pixel based classification model. LAI data were collected using manual measurements and a Licor LAI-2200C instrument which was operated according to the method explained by Danner et al. (2015).

The empirical model was trained on the Licor 2200C canopy analyser data using a linear combination of the inputs described above. The conceptual model was developed using only *VLADF* and products derived from drone-based images, without using any training data. The framework of the research is shown in Fig. 1.

2.1. Site description and data acquisition

The study was conducted on a maize crop (Scientific name: Zea mays L.; Variety: Cargil 900 M (gold)) in a research farm of the Agro Climate Research Centre, Professor Jayashankar Telangana State Agricultural University, Hyderabad, Telangana, India. The study area is a semi-arid region that lies between 17°19′27.2″N – 17°19′28.3″N and 78°23′55.4″E – 78°23′56.2″E as shown in Fig. 2(a). The data collection was undertaken from Nov 2018 to Feb 2020, including two winter growing seasons, locally known as *Rabi*. The research farm was divided into 4.2 m × 4.8 m subplots that were treated with three different water and nitrogen levels to enable the subplots to be at low, medium and high water and fertiliser stress conditions. The three different water and nitrogen treatments along with three replications of each treatment resulted in a total of 27 subplots, as shown in Fig. 2 (b). The plant spacing of 20 cm and row spacing of 60 cm of each subplot resulted in a plant density of ~8.33 plants per m^2. Table 1 shows the type of data collected from the farm.

Drone-based RGB images were captured periodically from a height of 25 m. An overlap of 70–80% at the front and 50–70% at the side was maintained in consecutive images captured by the drone-mounted camera. This overlap ensured creation of a quality orthomosaic (Raj et al., 2019). In the 2018–19 Rabi season, a 'Canon IXUS' camera was used, and in the Rabi 2019–20 season, a 'Micasense Altum' camera was used, because the Canon camera was damaged in the last flight of the 2018–19 season.

The LAI of each plot was recorded using a Licor 2200-C canopy analyser with a 270° view angle cap and three 'below' canopy readings per plot on the same day of each flight. Various canopy structural properties such as top leaf angle, leaf area and height of the canopy were also recorded during different growth stages. Five plants (four plants from the corners and one plant from the center) from each of the nine plots were chosen, and the area of every leaf calculated based on the lengths and widths of the leaves as shown in Fig. 3. No destructive sampling was done to record the lengths and widths of the leaves. The per-plant total leaf area of these five plants was averaged and multiplied with the number of plants in the respective plots. The total leaf area in a plot was then divided by the plot ground area, being 4.2 m × 4.8 m. The LAI calculated using this method was assumed to be the closest possible to the true LAI and termed LAI_{actual}.

2.2. Green-canopy cover, canopy height, and VLADF model creation

The airborne images were processed in the Agisoft® Metashape professional software to create an orthomosaic and to derive a DSM of the research farm (Ajayi et al., 2017). The data of the Rabi 2018–19 season were manually geotagged using ground control point coordinate information in the Agisoft software, for aligning the photos and creating a sparse point cloud. Subsequently, all unwanted areas from the farm point cloud were removed and only the area of interest retained for further processing. Later, dense point clouds were built and fed as input for creation of the farm orthomosaic and DSM for various dates. The orthomosaic and DSM were subsequently used to obtain the green crop cover (GCC) and the canopy height, respectively. GCC, canopy height and *VLADF* were fed as input to the LAI estimation models. The development of these three inputs is discussed in the following sections.

2.2.1. GCC estimation model

The orthomosaics created by Metashape® were imported into the

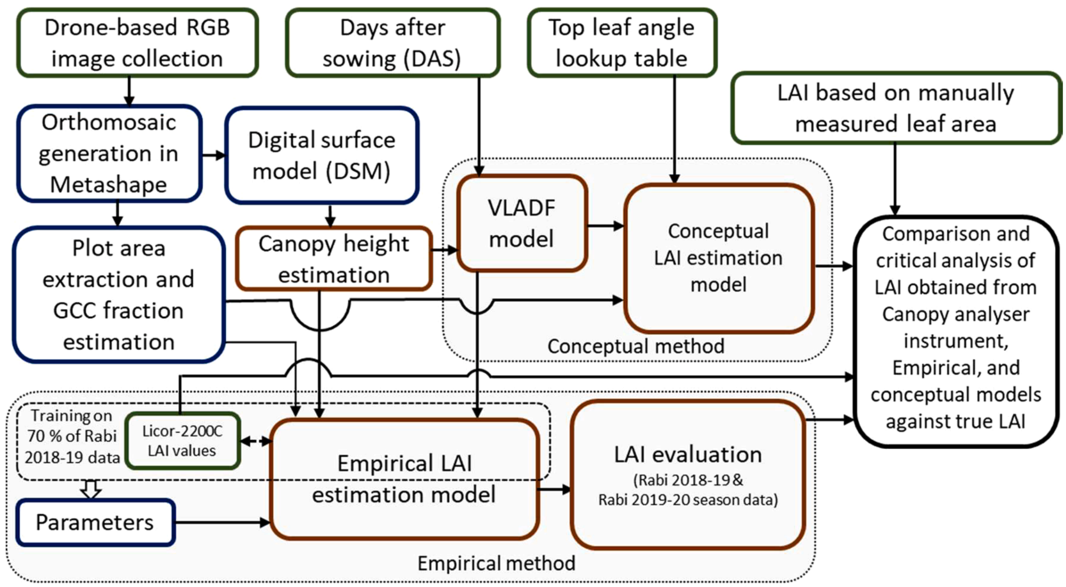

Fig. 1. Features derived from drone-based red-green-blue (RGB) data including canopy height and green-canopy cover (GCC) together with vertical leaf area distribution factor (*VLADF*) values (a lookup-table derived from canopy architectural properties data), are used as input to the LAI estimation models. The empirical LAI estimation model was trained with canopy analyser data, and results compared with the conceptual LAI estimation results, and with manually measured LAI from calculating the area of all the leaves. (For interpretation of the references to color in this figure legend, the reader is referred to the web version of this article.)

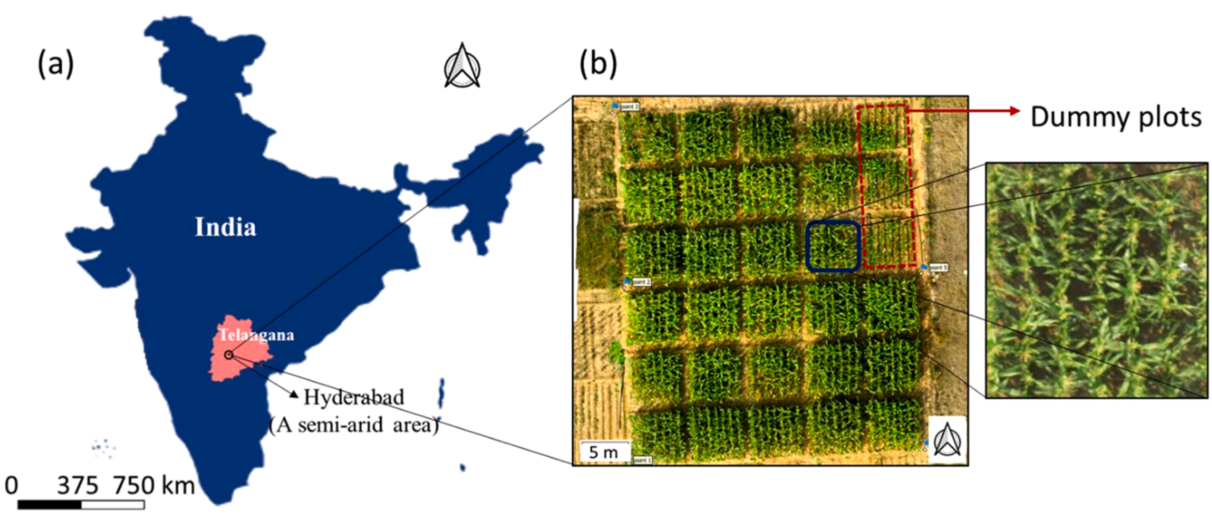

Fig. 2. (a) Geographical location of the farm, located in a semi-arid zone in the southern part of India. (b) Layout of the research farm as seen from the drone, which can capture leaf-level high-resolution (around 1 cm^2 pixel resolution) images.

QGIS® software, and every subplot extracted from the respective orthomosaic using a subplot shapefile. To estimate the GCC of subplots, the subplot RGB image was first converted into an HSV (hue/saturation/value) colour space. This colour space image was used for classification based on the colour of the object. In this image type, the hue channel was used to decide the colour type; the saturation channel represented shades of that colour; and the value channel represented the brightness of the colour. Using HSV images, the green pixels that represent the green-canopy were classified from each subplot as shown in Fig. 4 (a), and the GCC fraction calculated using

$$\textit{Green canopy cover fraction} = \frac{\text{number of green pixels in a subplot}}{\text{Total number of pixels in a subplot}}. \tag{1}$$

2.2.2. Canopy height estimation model

The DSM shown in Fig. 4 (b) was used as an input to the height estimation model. This DSM was exported from Metashape® as a TIFF file and imported into the QGIS® software. All the plots were cut out and analysed individually in QGIS®. The Otsu method (Otsu, 1979) was then used to separate all the pixels that represent the canopy area in individual plots.

Fig. 5 represents the process of estimating the canopy height from the cropped DSM of the individual plot. Fig. 5(a) is the DSM of one of the plots (plot number 27) for 19 Dec 2018. The average of the lowest five percentile elevation in Fig. 5(a) was assumed to portray the ground elevation in that plot (Fig. 5(f)) using a histogram of the DSM (Fig. 5(b)). Since two classes were present (canopy and ground) in the DSM, two Gaussian curves were present in the histogram. The histogram was smoothed using the probability density function (Fig. 5(c)) with the elevation value at the peak of the canopy Gaussian curve assumed as the threshold to classify the canopy pixels from ground pixels. An example of the classified DSM is shown in Fig. 5(d), with the average canopy

Table 1
Data collected from the research farm and their respective uses in this research.

Data	Instrument used	Pixel size/ Number of samples per plot	Use of the data
High spatial and temporal resolution top-of-canopy RGB images	Hexacopter-mounted Canon IXUS (Rabi 2018–19 season), and Micasense Altum (Rabi 2019–20 season)	Pixel size <2 cm	Input for remote estimation of the crop height and the green-canopy cover fraction
Foliage LAI	Licor Canopy analyser Model: 2200-C	Three 'below' canopy readings per plot, and frequent readings for atmospheric correction	Training of the LAI Model
Canopy height	Metre scale	An average height of five plants per plot is used to represent the height of the canopy of one plot	Used as ground truth data to validate the height estimation model
Top leaf angle	Clinometer mobile application	Leaf angles of top 5–6 leaves from five plants per plot	Used to create the *VLADF* model
True LAI	The lengths and widths of leaves were measured using a scale, as shown in Fig. 3	Five plants per plot for nine plots are recorded (one time)	To calculate the actual LAI of the plot for validation of all of the LAI models

elevation found by averaging all the pixel values above the T° threshold height (Fig. 5(e)), and the estimated height of the canopy calculated by subtracting ground elevation from canopy elevation (Fig. 5(g)).

This method was applied to all of the plots for all orthomosaic's over the study period. This method yielded an RMSE of 10 cm for the initial growth stages and an RMSE of around 20 cm for the maturity stage. The error in estimated canopy height was considered acceptable because the ground truth height against which it was compared had a standard deviation of ~15 cm for the crop at the silking stage. The analysis result of the canopy height estimation model is shown in Fig. 6.

2.2.3. *VLADF model*

The *VLADF* model developed here uses the crop sowing date and canopy height to provide a factor which relates canopy total leaf area to top-of-canopy leaf area visible from the drone-based image. A lookup table created for use with this model was subsequently used for estimating the maize LAI from drone-based top-of-canopy RGB images without requiring any further ground data collection.

The camera mounted on the drone can only see the ground-projected leaf area of the top-of-canopy leaves, as illustrated in Fig. 7. The average top leaf angle value can be used to convert this projected area into the actual top leaf area using

$$Top\ \ of\ \ the\ \ canopy\ \ leaf\ \ area = \frac{\text{Projected leaf area (A)}}{\text{Sin}\theta}. \tag{2}$$

The average leaf angle value can be noted from the farm at the time of flying the drone (using a clinometer), or taken from the graph in Fig. 8 (a), created in this research from the farm data collected during the Rabi 2018–19 and 2019–20 seasons. It should be noted that the standard deviation of the average top leaf angle at different growth stages was between 7° (for the initial growth stages) and 12° (for the later growth

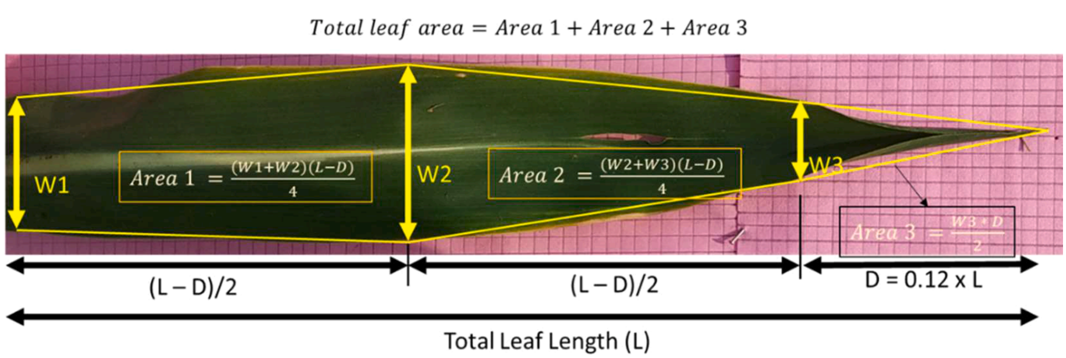

Fig. 3. Calculation of the actual area of a leaf by using the length and width of the leaf, measured at different locations. Area is calculated based on the geometric formulae shown.

Fig. 4. (a) Image thresholding using the hue, saturation and value (HSV) method to calculate the green-canopy cover fraction, as seen from a top-of-the-canopy image; and (b) digital surface model (DSM) of the plot made from 7 Jan 2019 RGB images. (For interpretation of the references to color in this figure legend, the reader is referred to the web version of this article.)

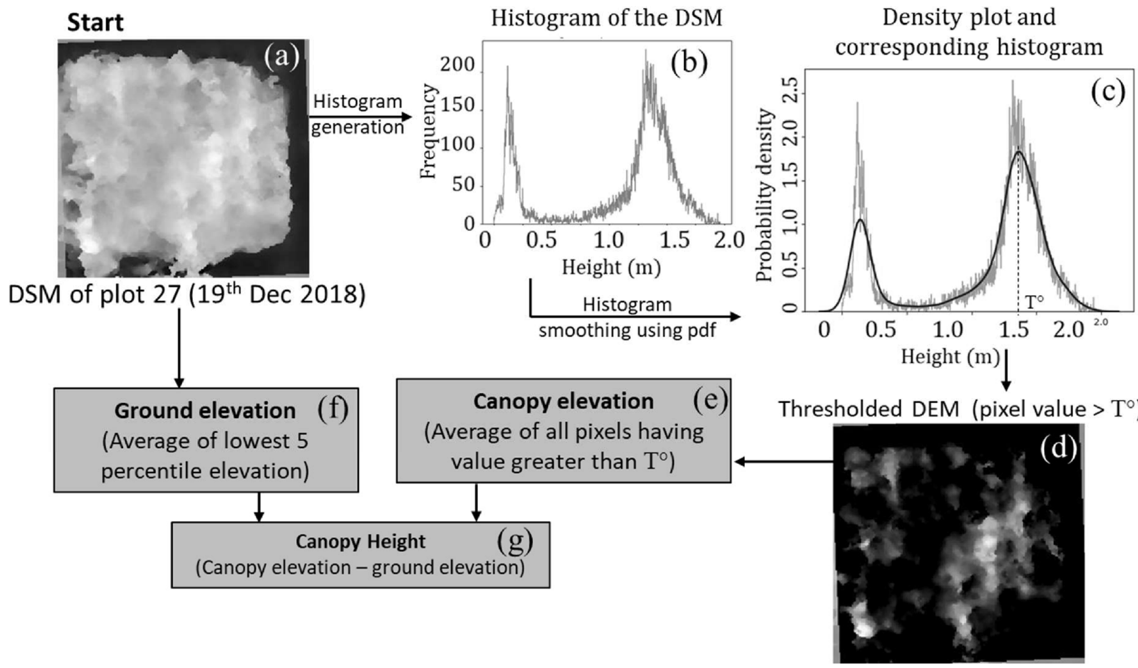

Fig. 5. Framework for estimating canopy height from plot-level digital surface model (DSM). Histogram of the plot-level DSM is used to classify the canopy and background pixels. The height at which the peak of the canopy class is observed is selected as the threshold to separate high canopy pixels. The average of these high elevation pixels (considered as top of canopy pixels) is then subtracted from the lowest five percentile elevation pixels (considered as ground elevation) to obtain the canopy height of the plot.

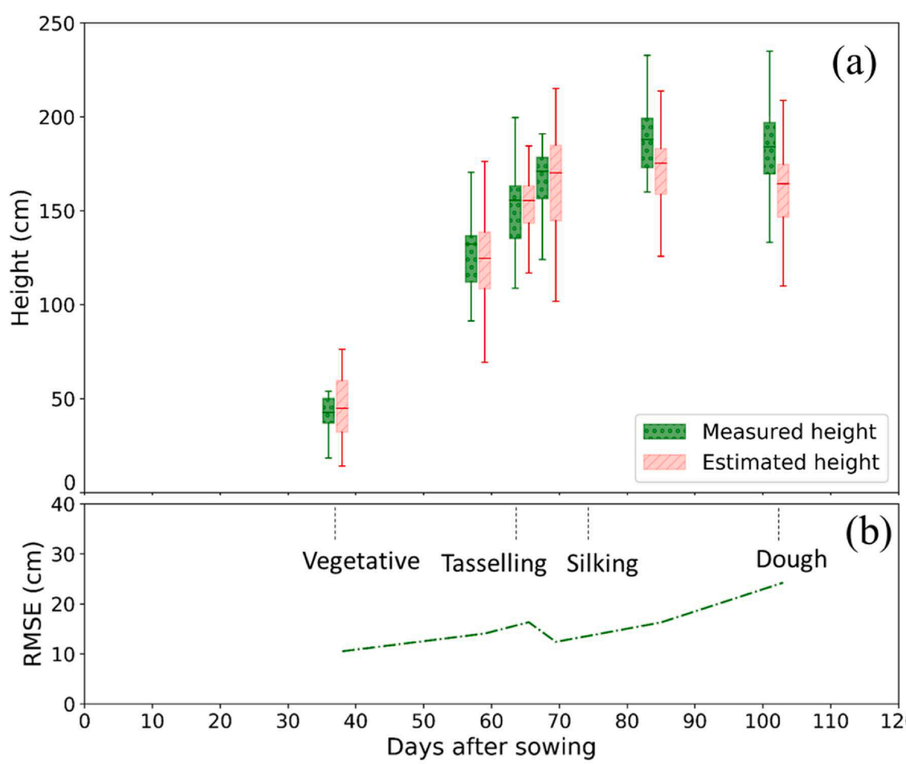

Fig. 6. (a) Box-whisker plot of measured and estimated canopy heights where the centre part (box) represents the middle 50 percentile of the data set (horizontal line in the box represents median value) and the whiskers represent the lower and upper quartile of the data, and (b) RMSE of the estimated canopy height.

stages). The lengths and the widths of the leaves along with the leaf angles were calculated to determine the actual leaf area in a plant. This information was used to develop the *VLADF*, and to compare the estimated LAI with the actual/true LAI.

In developing the *VLADF*, information about the leaf area (collected from the data of the Rabi 2018–19 season) were used to relate the top-of-canopy leaf area with the full canopy leaf area. The following steps were used to determine the *VLADF*:

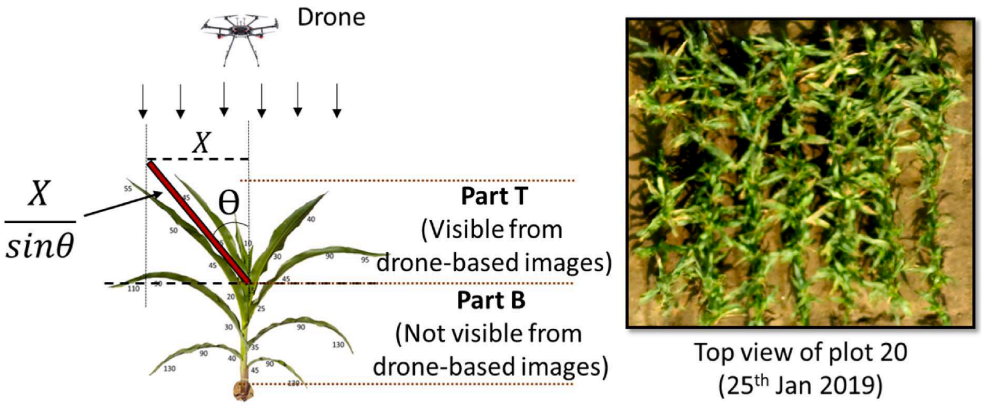

Fig. 7. Image representing the relationship between the projected top leaf area (X) - as approximated by the average of top leaves - to the actual top leaf area (X/Sinθ). The top part (T) of the canopy is visible from drone-based images, however the bottom part (B) of the canopy is not visible in the images. The complete leaf area that is based on the top section leaf area is therefore calculated by a factor obtained from the *VLADF*. As an example, the image to the right is a view of a plot in which the visible leaf area is the projected area.

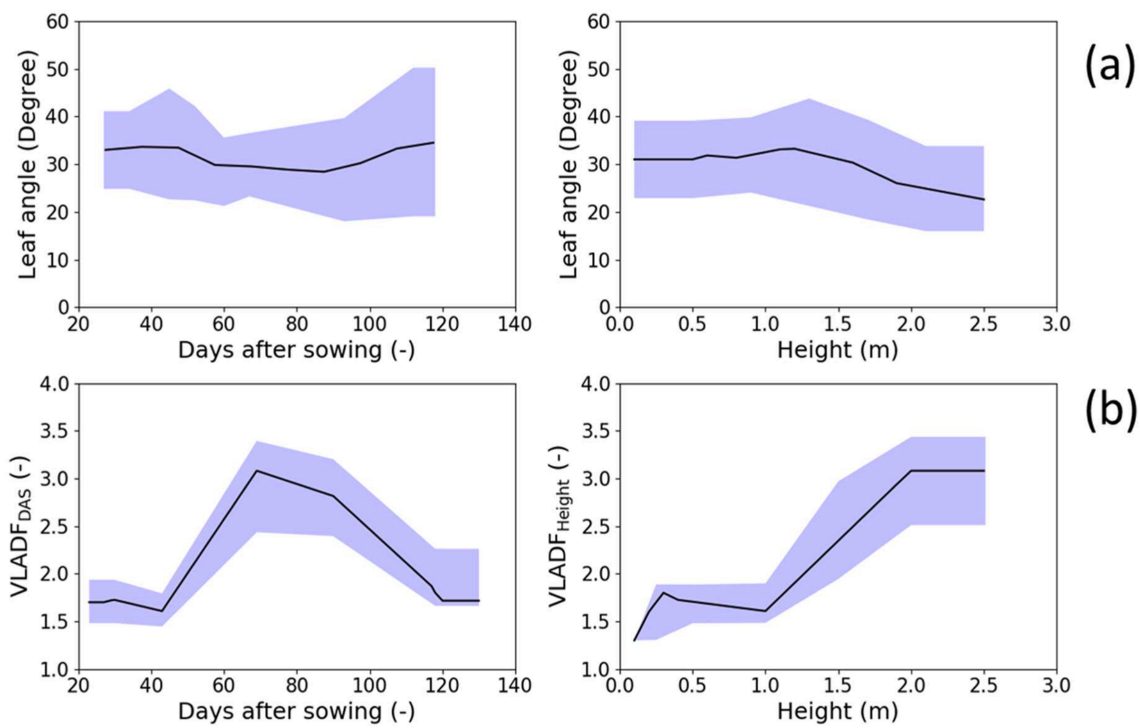

Fig. 8. (a) Top-of-canopy average leaf angle based on the days after sowing (DAS) and the canopy height; (b) A *VLADF* graph based on the DAS and the canopy height. The graphs are used as lookup table to find the average *VLADF* factor for a canopy which is based on height and age of the crops. The shaded area represents uncertainity of the values within 75% confidence limits as approximated by $\pm 1.15{*}SD$ of the dataset.

(i) Divide the vertical profile of the plant into two sections based on the height and the age of the plant (Days after Sowing - DAS). The top section depth is determined based on the depth that is captured by the drone-based camera. The top part of the plant is denoted by T, and the bottom part is denoted by B (Fig. 7).
(ii) Find the total leaf area of part T ($area_T$) and part B ($area_B$). Scale the leaf area of part T to 'one' and, accordingly, find the factor for the leaf area of part B separately for height and DAS-based analysis. The separate calculation of *VLADF* for height and DAS is vital, because at the same DAS plants can have different heights.
(iii) The final value of *VLADF* is obtained after averaging the height- and DAS-based *VLADF* by using

$$VLADF_{height} = 1 + \frac{area_B}{area_T} \quad (3)$$

$$VLADF_{DAS} = 1 + \frac{area_B}{area_T} \quad (4)$$

$$VLADF = \frac{VLADF_{height} + VLADF_{DAS}}{2} \quad (5)$$

The *VLADF* values used were from a lookup table based on the graph shown in Fig. 8 (b) (created from the data of 2018–19 Rabi season). If the DAS is known it can be directly used in the model; otherwise techniques such as those explained in Sadeh et al. (2019) can be used to estimate the DAS information.

Same DAS crop can have a different canopy height depending on the input resources provided to the crop. Moreover, once the crop reaches canopy closure (mostly after flowering/tasseling stage) the number of leaves and area of the leaves stops growing. As the crop moves towards the maturity stage, the leaves start drying and the total leaf area starts decreasing. During the tasseling-silking stage, the maize canopy structure becomes consistent with slightly decreasing nature of VLADF. The relatively consistent leaf area during the tasseling-silking stage resulted in the approximately same $VLADF_{DAS}$ values around DAS 80. The lookup table (graphically shown in Fig. 8) can be used for any future VLADF value determination and ground-truth data related to canopy height, leaf area, and leaf angle need not be collected again..

The input of DAS to the *VLADF* model acts as a proxy indicator of the leaf area changes with respect to growth stage of the crop. The *VLADF* model also incorporates the fact that canopies in the same growth stage can be of different heights with different vertical leaf area distributions. Therefore, the average of the height and the DAS-based factors is taken as the *VLADF* value to be used. This proposed *VLADF* model can be used for all maize cultivars having similar growing degree day (GDD) characteristics with no further field data collection needed for implementation of this model. To further improve the model, the DAS could be replaced with GDD. However, in that case the farm-level diurnal atmospheric temperature is required to calculate the GDD.

2.3. The LAI estimation models

2.3.1. Empirical model

The empirical LAI estimation model developed in this paper used the estimated canopy height, GCC, and the *VLADF* as input. These three inputs capture all of the physical parameters that can impact the LAI of the canopy. However, the contribution of GCC to the model is insignificant when the top-of-canopy leaf area is saturated due to canopy closure. The contribution of the canopy height is also minimal when the canopy reaches its maximum height for similar reasons. Accordingly, most of the existing models cannot perform well when these two parameters achieve their maximum limit, with values not changing much with further crop growth. The addition of the *VLADF* input to LAI estimation was hypothesized to improve the performance as *VLADF* incorporates the changes that occur inside the canopy, which cannot be captured from the airborne imagery of the top of the canopy. The framework of the LAI estimation model has already been shown in Fig. 1.

The model was trained to the Licor 2200-C LAI using a linear regression on 70% of the Rabi 2018–19 data (randomly sampled from every growth stage), tested on the remaining 30% of the Rabi 2018–19 data, and validated on the data from the Rabi 2019–20 season. The resulting model was

$$LAI_{empirical} = 1.15{*}GCC + 0.74{*}Canopy_{height} + 0.78{*}VLADF - 1.29, \tag{6}$$

where $LAI_{estimated}$ is the model output, *GCC* is the fraction of the green-canopy cover, $Canopy_{height}$ is the estimated canopy height from the DSMs of the farm and *VLADF* is vertical leaf area distribution factor.

2.3.2. Conceptual model

In contrast to the empirical model, the *VLADF* values were also used to independently calculate the LAI using the following conceptual construct

$$LAI_{conceptual} = VLADF{*}(Top\ \ of\ \ the\ \ canopy\ \ leaf\ \ area) = \frac{VLADF{*}GCC}{\sin(\theta)}, \tag{7}$$

where θ is the average top leaf angle of the crop, which can be taken from Fig. 8 (a) or measurements at the time of flying the drone. Here, *VLADF* is a multiplication factor which relates the top-of-canopy leaf area to total leaf area, dependent on DAS and canopy height. The top-of-canopy leaf area in this conceptual model is derived from GCC, being the horizontal projection of leaf area as seen from the drone camera (Fig. 7). The actual top-of-canopy leaf area is obtained from the plant geometry by dividing GCC with the sine of the average leaf angle. Once the actual leaf area of the top-of-canopy is estimated it is multiplied by the *VLADF* to obtain the full canopy leaf area. This method was tested against the one-time true leaf area index measurements of the nine plots (combination of three different levels of irrigation and fertiliser treatments).

3. Results

The *VLADF* relationships developed from the Rabi 2018–19 crop structural parameters data were evaluated for the Rabi 2019–20 season data, using the detailed plant structural parameters recorded from the nine sub-plots at 93 DAS of the Rabi 2019–20 season crop. The height of the nine sub-plot canopies ranged between 138 cm and 219 cm. Based on the estimated height and the DAS of these nine plots, VLADF was calculated using the relationships in Fig. 8. The region between higher and lower limit lines (Fig. 9) shows the '(model VLADF)±(1.15*SD)' region for 93 DAS, where SD is standard deviation. The multiplier value of '1.15' was used to represent a confidence interval of 75%. Only one value was substantially outside the expected range with all other plots within an acceptable range.

The empirical LAI estimation correlated with the LAI values from the canopy analyser with a coefficient of determination (R^2) of 0.84 and 0.77, and an RMSE of 0.36 and 0.45 on the test (30% of Rabi 2018–19) and the validation (Rabi 2019–20) data, respectively. These RMSE values can be considered low because the canopy analyser instrument itself has a standard deviation of 0.2 for the same location data (calculated by taking repeated canopy analyser readings from the same location). However, a slight overestimation of the LAI for the early growth stage of the crop and an underestimation for the late growth stage of the plants was also found for validation dataset (Fig. 10).

While the empirical model presented here has shown comparatively good results relative to other studies when evaluated with Licor canopy analyser data, comparison with the true LAI values showed a coefficient of determination of only 0.56 and an RMSE of 1.34 (Fig. 11(b)). In contrast, the conceptual LAI estimation correlated with the true LAI from measurements yielded an improved coefficient of determination of 0.59 with an RMSE of 0.73 (Fig. 11(a)).

4. Discussion

The models created in this research can be used for foliage LAI (empirical model) as well as true LAI estimation (conceptual model) of maize crops. For any other crop, the VLADF lookup-table first needs to be created following the approach outlined in this research. While the empirical model would first require recalibration for foliage LAI estimation, the conceptual model can be used directly for true LAI estimation. Fig. 12 shows the flowchart of how this research can be implemented for any other data.

The results from this paper, particularly the deviation from true values is better than the results of other published models, including Delegido et al. (2013) which used the spaceborne red-edge index to estimate LAI of multiple crops including maize with an R^2 of 0.82 and RMSE of 0.6 when compared with Licor LAI-2000 values. While Haboudane et al. (2004) used more costly drone-based hyperspectral data to estimate LAI with a modified triangular vegetation index (MTVI2) and modified chlorophyll absorption ratio index (MCARI2) developed from empirical analysis of the PROSPECT and SAILH models; an R^2 of 0.89 and RMSE of 0.46 was achieved for maize crop when tested on the same season data. Moreover, Jay et al. (2017) achieved an R^2 of 0.89 and RMSE of 0.23 for sugar beet crops for LAI estimation till the vegetative stage, using an index based approach with UAV-based multispectral data. When considering the same growth stage as used in Jay et al. (2017), the model developed in this research has shown similar results by achieving an R^2 of 0.91 and RMSE 0.29. Moreover, when using the more complex PROSAIL inversion model for LAI estimation, Jay et al. (2017) only achieved an R^2 between 0.68 and 0.81 and RMSE of 0.39–0.72. Importantly, the multispectral data based LAI model cited here only used vegetative stage data to check the performance of the model, but canopy closure occurs after the vegetative stage, where these models show insensitivity towards changes in leaf area at the bottom of the canopy. Moreover, PROSAIL is a point data simulation model and does not give spatial variability. Further, application of these indices

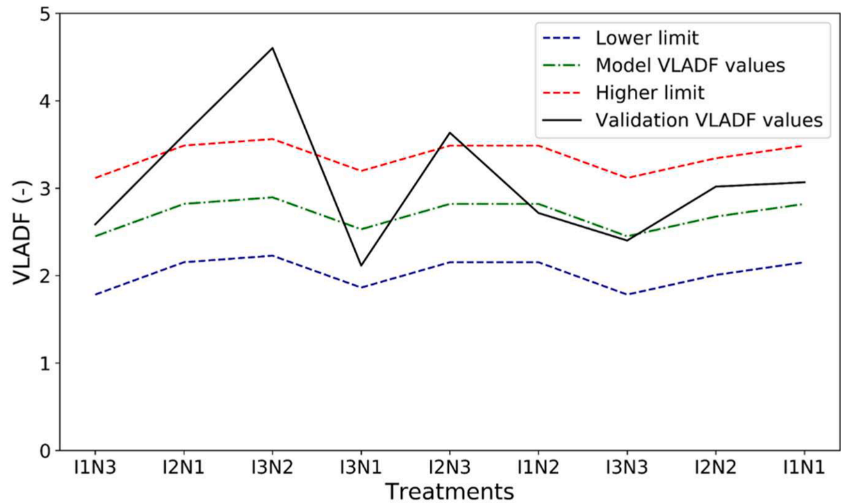

Fig. 9. Evaluation result of the *VLADF* model for canopies at 93 days after sowing. IxNx on the x-axis represents plots with different irrigation (I) and nitrogen (N) treatments. I1N1 stands for low irrigation and fertilisation and while I3N3 represents high irrigation and fertilisation. The model performance was found to be within the tolerable limits.

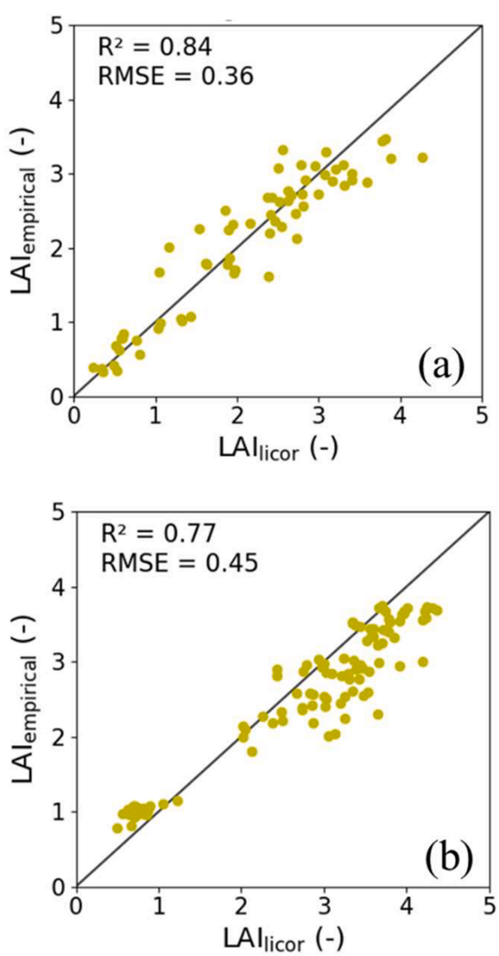

Fig. 10. Scatterplots representing the results of the empirical LAI model on (a) test (30% of Rabi 2018–19) and (b) validation (100% of Rabi 2019–20) data.

methods and PROSAIL require a more costly multispectral and hyperspectral data, respectively. In contrast, the model developed in this paper uses data from a simple and cheap RGB camera while achieving better or similar accuracy, even in the case of reproductive growth stages where canopy closure effects the derived LAI.

Results of the conceptual allometric model created in this resaech can be contrasted with the allometric model of Colaizzi et al. (2017), which used a calibrated log normal function by considering cumulative growing degree days, canopy height, and plant population as model inputs, collected through field sensors and manual field observations. Using destructive sampling to calculate the true LAI of the canopy, an R^2 of 0.54 and RMSE of 1.14 was achieved for maize crop LAI.

As shown in Fig. 11(c) Licor-based LAI values are reliable only until the vegetative stage of the crop, being when the LAI of the canopy is low. Once the LAI of the canopy increases above 4, the Licor-based measurements of LAI start saturating. Similar observations were noted by Smith et al. (1993) and Cutini et al. (1998), where the LAI 2000 canopy analyser consistently underestimated canopy LAI. This problem of underprediction is majorly due to the assumption that leaves of the canopy are randomly distributed, which is not valid in many cases (Breda, 2003; Gower et al., 1999). However, It should also be noted that LAI estimated from Licor-2200C measurements represent the foliage area index, which gets affected by stem and other non-green plant elements. In contrast, the conceptual LAI model proposed here considers only leaf area, thus more correctly representing the true leaf area index.

5. Conclusion

Two models for estimation of leaf area index from top-of-canopy images were developed and evaluated in this research. The first, an empirical model trained and tested on Licor canopy analyser data, was found to have a higher R^2 and lower RMSE values than existing farm-level remote sensing based LAI estimation techniques. But as this model was trained on Licor canopy analyser data it is more representative of foliage area index and thus had a poor estimation of the leaf area index derived from manual measurements. The second model was based on the conceptual use of a VLADF (vertical leaf area distribution factor), estimated through allometric properties of the canopy, to relate top-of-canopy leaf area to full canopy leaf area for different growth stages and heights of the crop. This has enabled the changes within the canopy to be captured even during canopy closure (i.e. post tasselling stage). This new model can therefore be used for analysing spatial and temporal LAI changes across farms in near real-time with an R^2 of ~ 0.6 and RMSE of 0.73 when compared to independent manual measurements.

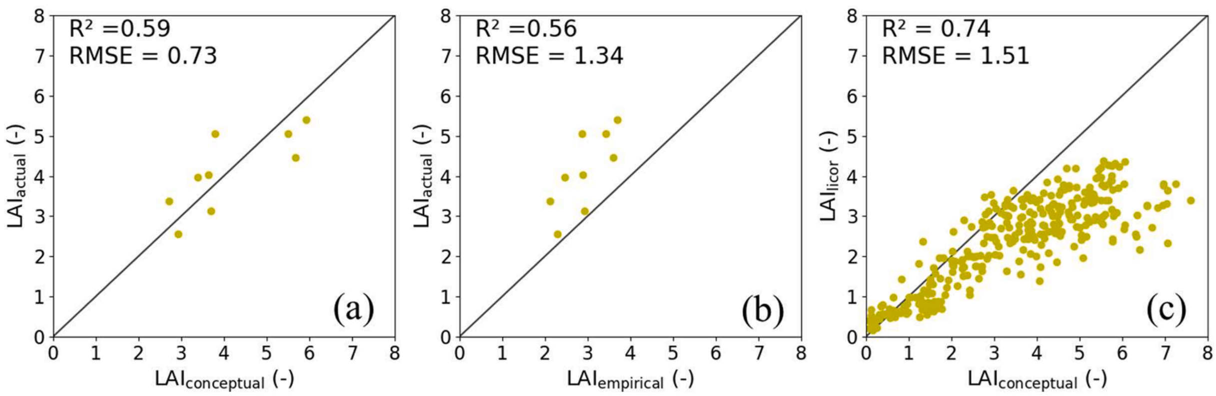

Fig. 11. Comparison of the LAI estimates from the (a) Conceptual $LAI_{conceptual}$ against manual measurements LAI_{actual}; (b) Empirical $LAI_{empirical}$ against the manual measurements LAI_{actual}; and; (c) Canopy analyser based LAI_{licor} against the conceptual $LAI_{conceptual}$.

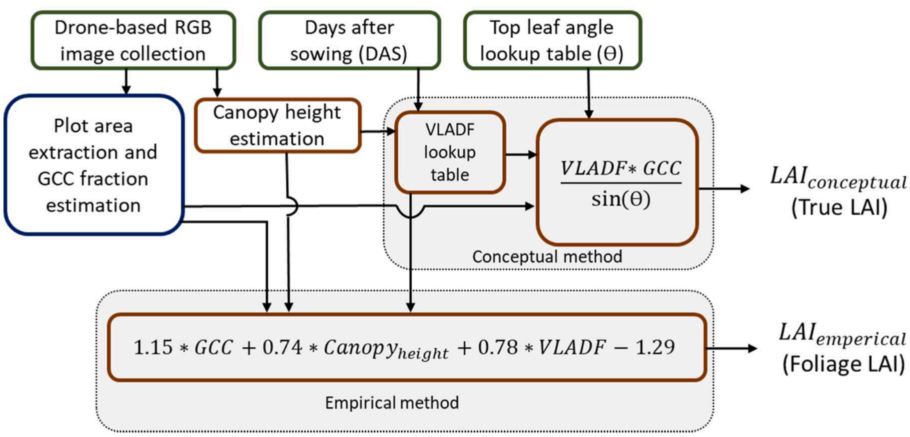

Fig. 12. Flowchart for application of true and foliage LAI estimation models. Green canopy cover (GCC) and canopy height can be estimated from the drone-based RGB data. Top leaf angle information for the maize crop can be used from the lookup table given in Fig. 8(a) while the VLADF for a maize crop can be obtained from Fig. 8(b). For any other crop, another lookup table for VLADF needs to be created in the same way as proposed in Section 2.2.3. These information can be used to obtain true and foliage LAI following the equations shown in the conceptual and empirical blocks, respectively. The empirical model equation is only valid for maize crop, though it can be applied to any other crop provided model training is undertaken. (For interpretation of the references to color in this figure legend, the reader is referred to the web version of this article.)

Funding

This research was jointly funded by the Department of Science and Technology (DST); Ministry of Science and Technology, Government of India; and Japan Science and Technology (JST), Government of Japan (DST/INT/JST/P-29/2016). IITB-Monash Research Academy has funded the resources used in the research.

CRediT authorship contribution statement

Rahul Raj: Conceptualization, Methodology, Formal analysis, Visualization, Validation. **Jeffrey P. Walker:** Conceptualization, Investigation, Resources, Supervision. **Rohit Pingale:** Validation, Data curation, Visualization. **Rohit Nandan:** Conceptualization. **Balaji Naik:** Conceptualization, Validation, Resources. **Adinarayana Jagarlapudi:** Investigation, Resources, Supervision, Project administration, Funding acquisition.

Declaration of Competing Interest

The authors declare that they have no known competing financial interests or personal relationships that could have appeared to influence the work reported in this paper.

Acknowledgements

The authors would like to acknowledge BharatRohan company for their help in flying the drone for data collection and Professor Jayashankar Telangana State Agricultural University for providing the farm test-bed for carrying out the research. The critical reviews and suggestions during project progress presentations from all the members of the DST-JST project has refined this study and helped in achieving better results.

References

AgiSoft PhotoScan Professional (Version 1.2.6) (Software), 2016. Retrieved from http://www.agisoft.com/downloads/installer/.

Ajayi, O.G., Salubi, A.A., Angbas, A.F., Odigure, M.G., 2017. Generation of accurate digital elevation models from UAV acquired low percentage overlapping images. Int. J. Remote Sens. 38 (8–10), 3113–3134.

Behera, S.K., Srivastava, P., Pathre, U.V., Tuli, R., 2010. An indirect method of estimating leaf area index in Jatropha curcas L. using LAI-2000 Plant Canopy Analyzer. Agric. For. Meteorol. 150 (2), 307–311.

Bendig, J., Yu, K., Aasen, H., Bolten, A., Bennertz, S., Broscheit, J., Gnyp, M.L., Bareth, G., 2015. Combining UAV-based plant height from crop surface models, visible, and near infrared vegetation indices for biomass monitoring in barley. Int. J. Appl. Earth Obs. Geoinf. 39, 79–87.

Bonan, G.B., 1993. Importance of leaf area index and forest type when estimating photosynthesis in boreal forests. Remote Sens. Environ. 43 (3), 303–314.

Breda, N.J., 2003. Ground-based measurements of leaf area index: a review of methods, instruments and current controversies. J. Exp. Bot. 54 (392), 2403–2417.

Bryson, R.J., Paveley, N.D., Clark, W.S., Sylvester-Bradley, R., Scott, R.K., 1997. Use of in-field measurements of green leaf area and incident radiation to estimate the effects of yellow rust epidemics on the yield of winter wheat. In: Developments in Crop Science, Vol. 25. Elsevier, pp. 77–86.

Chen, J.M., Black, T.A., 1991. Measuring leaf area index of plant canopies with branch architecture. Agric. For. Meteorol. 57 (1–3), 1–12.

Chen, J.M., Black, T.A., 1992. Defining leaf area index for non-flat leaves. Plant, Cell Environ. 15 (4), 421–429.

Colaizzi, P.D., Evett, S.R., Brauer, D.K., Howell, T.A., Tolk, J.A., Copeland, K.S., 2017. Allometric method to estimate leaf area index for row crops. Agron. J. 109 (3), 883–894.

Cutini, A., Matteucci, G., Mugnozza, G.S., 1998. Estimation of leaf area index with the Li-Cor LAI 2000 in deciduous forests. For. Ecol. Manage. 105 (1–3), 55–65.

Danner, M., Locherer, M., Hank, T., Richter, K., EnMAP Consortium, 2015. Measuring Leaf Area Index (LAI) with the LI-Cor LAI 2200C or LAI-2200 (+ 2200Clear Kit)–theory, measurement, problems, interpretation.

Delegido, J., Verrelst, J., Meza, C.M., Rivera, J.P., Alonso, L., Moreno, J., 2013. A red-edge spectral index for remote sensing estimation of green LAI over agroecosystems. Eur. J. Agron. 46, 42–52.

Drewry, D.T., Kumar, P., Long, S., Bernacchi, C., Liang, X.Z., Sivapalan, M., 2010. Ecohydrological responses of dense canopies to environmental variability: 1. Interplay between vertical structure and photosynthetic pathway. J. Geophys. Res. Biogeosci. 115 (G4).

Duan, B., Liu, Y., Gong, Y., et al., 2019. Remote estimation of rice LAI based on Fourier spectrum texture from UAV image. Plant Methods 15, 124. https://doi.org/10.1186/s13007-019-0507-8.

Dufrêne, E., Bréda, N., 1995. Estimation of deciduous forest leaf area index using direct and indirect methods. Oecologia 104 (2), 156–162.

Fassnacht, K.S., Gower, S.T., Norman, J.M., McMurtric, R.E., 1994. A comparison of optical and direct methods for estimating foliage surface area index in forests. Agric. For. Meteorol. 71 (1–2), 183–207.

Garrigues, S., Shabanov, N.V., Swanson, K., Morisette, J.T., Baret, F., Myneni, R.B., 2008. Intercomparison and sensitivity analysis of Leaf Area Index retrievals from LAI-2000, AccuPAR, and digital hemispherical photography over croplands. Agric. For. Meteorol. 148 (8–9), 1193–1209.

Gower, S.T., Kucharik, C.J., Norman, J.M., 1999. Direct and indirect estimation of leaf area index, fAPAR, and net primary production of terrestrial ecosystems. Remote Sens. Environ. 70 (1), 29–51.

Haboudane, D., Miller, J.R., Pattey, E., Zarco-Tejada, P.J., Strachan, I.B., 2004. Hyperspectral vegetation indices and novel algorithms for predicting green LAI of crop canopies: modeling and validation in the context of precision agriculture. Remote Sens. Environ. 90 (3), 337–352.

Jay, S., Maupas, F., Bendoula, R., Gorretta, N., 2017. Retrieving LAI, chlorophyll and nitrogen contents in sugar beet crops from multi-angular optical remote sensing: Comparison of vegetation indices and PROSAIL inversion for field phenotyping. Field Crops Res. 210, 33–46.

Kimm, H., Guan, K., Jiang, C., Peng, B., Gentry, L.F., Wilkin, S.C., Wang, S., Cai, Y., Bernacchi, C.J., Peng, J., Luo, Y., 2020. Deriving high-spatiotemporal-resolution leaf area index for agroecosystems in the US Corn Belt using Planet Labs CubeSat and STAIR fusion data. Remote Sens. Environ. 239, 111615.

Li, S., Yuan, F., Ata-UI-Karim, S.T., Zheng, H., Cheng, T., Liu, X., Tian, Y., Zhu, Y., Cao, W., Cao, Q., 2019. Combining color indices and textures of UAV-based digital imagery for rice LAI estimation. Remote Sens. 11 (15), 1763.

Liu, J., Pattey, E., 2010. Retrieval of leaf area index from top-of-canopy digital photography over agricultural crops. Agric. For. Meteorol. 150 (11), 1485–1490.

Martin, K.L., Girma, K., Freeman, K.W., Teal, R.K., Tubańa, B., Arnall, D.B., Chung, B., Walsh, O., Solie, J.B., Stone, M.L., Raun, W.R., 2007. Expression of variability in corn as influenced by growth stage using optical sensor measurements. Agron. J. 99 (2), 384–389.

Mathews, A.J., Jensen, J.L., 2013. Visualizing and quantifying vineyard canopy LAI using an unmanned aerial vehicle (UAV) collected high density structure from motion point cloud. Remote Sens. 5 (5), 2164–2183.

Otsu, N., 1979. A threshold selection method from gray-level histograms. IEEE Trans. Syst. Man Cybernet. 9 (1), 62–66.

Patanè, C., 2011. Leaf area index, leaf transpiration and stomatal conductance as affected by soil water deficit and VPD in processing tomato in semi arid Mediterranean climate. J. Agron. Crop Sci. 197 (3), 165–176.

Qu, Y., Meng, J., Wan, H., Li, Y., 2016. Preliminary study on integrated wireless smart terminals for leaf area index measurement. Comput. Electron. Agric. 129, 56–65.

Raj, R., Suradhaniwar, S., Nandan, R., Jagarlapudi, A., Walker, J., 2019. Drone-based sensing for leaf area index estimation of citrus canopy. In: International Conference on Unmanned Aerial System in Geomatics. Springer, Cham, pp. 79–89.

Raj, R., Kar, S., Nandan, R., Jagarlapudi, A., 2020. Precision agriculture and unmanned aerial vehicles (UAVs). In: Unmanned Aerial Vehicle: Applications in Agriculture and Environment. Springer, Cham, pp. 7–23.

Raychaudhuri, B., Bhattacharyya, S., 2007. Temporal change in canopy reflectance at visible wavelength as a biophysical indicator of jute (Corchorus capsularis L.) growth. Int. J. Remote Sens. 28 (23), 5237–5253.

Running, S.W., Coughlan, J.C., 1988. A general model of forest ecosystem processes for regional applications I. Hydrologic balance, canopy gas exchange and primary production processes. Ecol. Model. 42 (2), 125–154.

Sadeh, Y., Zhu, X., Chenu, K., Dunkerley, D., 2019. Sowing date detection at the field scale using CubeSats remote sensing. Comput. Electron. Agric. 157, 568–580.

Smith, N.J., Chen, J.M., Black, T.A., 1993. Effects of clumping on estimates of stand leaf area index using the LI-COR LAI-2000. Can. J. For. Res. 23 (9), 1940–1943.

Stroppiana, D., Boschetti, M., Confalonieri, R., Bocchi, S., Brivio, P.A., 2006. Evaluation of LAI-2000 for leaf area index monitoring in paddy rice. Field Crops Res. 99 (2–3), 167–170.

Tao, H., Feng, H., Xu, L., Miao, M., Long, H., Yue, J., Li, Z., Yang, G., Yang, X., Fan, L., 2020. Estimation of crop growth parameters using UAV-based hyperspectral remote sensing data. Sensors 20 (5), 1296.

Tian, J., Wang, L., Li, X., Gong, H., Shi, C., Zhong, R., Liu, X., 2017. Comparison of UAV and WorldView-2 imagery for mapping leaf area index of mangrove forest. Int. J. Appl. Earth Obs. Geoinf. 61, 22–31.

Valentinuz, O.R., Tollenaar, M., 2004. Vertical profile of leaf senescence during the grain-filling period in older and newer maize hybrids. Crop Sci. 44 (3), 827–834.

Vose, J.M., Dougherty, P.M., Long, J.N., Smith, F.W., Gholz, H.L., Curran, P.J., 1994. Factors influencing the amount and distribution of leaf area of pine stands. Ecol. Bull. 102–114.